Tectonophysics, 82 (1982) 57–68
Elsevier Scientific Publishing Company, Amsterdam—Printed in The Netherlands

SEISMIC INVESTIGATIONS OF THE NANSEN RIDGE DURING THE FRAM I EXPERIMENT

Y. KRISTOFFERSEN [1], E.S. HUSEBYE [2,3], H. BUNGUM [2] AND S. GREGERSEN [4]

[1] *Norwegian Polar Research Institute, Oslo (Norway)*
[2] *NTNF/NORSAR, Kjeller (Norway)*
[3] *Depts. of Geology and Geophysics, University of Oslo, Oslo (Norway)*
[4] *Geodetical Institute, Copenhagen (Denmark)*

(Received January 1, 1981; revised version accepted May 6, 1981)

ABSTRACT

Kristoffersen, Y., Husebye, E.S., Bungum, H. and Gregersen, S., 1982. Seismic investigations of the Nansen Ridge during the FRAM I experiment. *Tectonophysics*, 82: 57–68.

As part of the FRAM I ice station experiment in the Arctic Ocean during the period March 11–May 15, 1979, a sonobuoy array was kept in operation for about 6 weeks. During the last two days of the experiment the array drifted over the crestal mountains of the western flank of the Nansen Ridge. Here microearthquakes were recorded at a rate of 1–2 events per hour, with epicentral distances from 15 to 25 km. Two parallel epicenter lineations are found, a main one that coincides with the median valley and another less active one that follows the northwestern rift-valley wall. This activity may be related to the uplift of a fault block from the median valley onto the rift valley wall. A crustal model for the crestal mountain area was obtained from two unreversed refraction profiles, giving preliminary compressional velocities of 4.6 km/s at the sea floor, a 6.1 km/s refractor at 1.5 km depth, and a 7.9 km/s refractor at 6 km depth, while in the median valley a 7.2 km/s refractor is found at a depth of 3 km.

INTRODUCTION

Our main sources of information about the Nansen Ridge—the active spreading center in the Arctic Ocean—are the teleseismically recorded earthquakes (Sykes, 1965; Barazangi and Dorman, 1970) and the aeromagnetic surveys reported by Karasik (1968) and Vogt et al. (1979a). Continuous bathymetric data have only been collected on a small number of submarine traverses across the ridge (Beal, 1969; Feden et al., 1979). Sea-floor spreading at the Nansen Ridge was probably initiated concurrently with the opening of the Norwegian–Greenland Sea and no major fracture zones have been located along the length of the ridge (Vogt et al., 1979b). Large regional variations in the depth of the rift valley floor and the amplitude of the central magnetic anomaly are observed along the Nansen Ridge, notably in the western part (Feden et al., 1979).

As part of a long-term effort to improve our knowledge of the Eurasian part of

0040-1951/82/0000–0000/$02.75

the Arctic, U.S. ice station FRAM I with participating scientists from Canada, Denmark and Norway was deployed on an ice floe in the Arctic Ocean north of Greenland from March 11–May 15, 1979. The ice station drifted southeast from the abyssal plain east of Morris Jessup Rise (84°50′N 10°W) towards the axis of the Trans Arctic Nansen Ridge (83°19′N 07°W) where it was abandoned. The drift path shown in Fig. 1 covered a total distance of 160 n.m. The thickness of the ice floe was 2.5 m and water depths ranged from 4100 to 2290 m.

The geophysics program on FRAM I encompassed: bathymetry, gravity, seismic reflection profiling, refraction measurements, microearthquake monitoring and underwater acoustics. Helicopter-borne geophysical surveys were carried out to 50 km distance from the camp. Other programs were regional oceanographic measurements, meteorology, marine biology and polar-bear studies (Hunkins et al., 1979).

This paper reports on the seismicity of the Nansen Ridge as recorded by a sonobuoy array during the drift of FRAM I. Complementary spot-depth soundings and seismic refraction measurements were also made to delineate to bathymetry and obtain a crustal seismic velocity model for the western flank of the Nansen Ridge. Results of the seismic refraction program will be reported in a separate paper and only preliminary results of the two refraction lines closest to the rift axis are reported here.

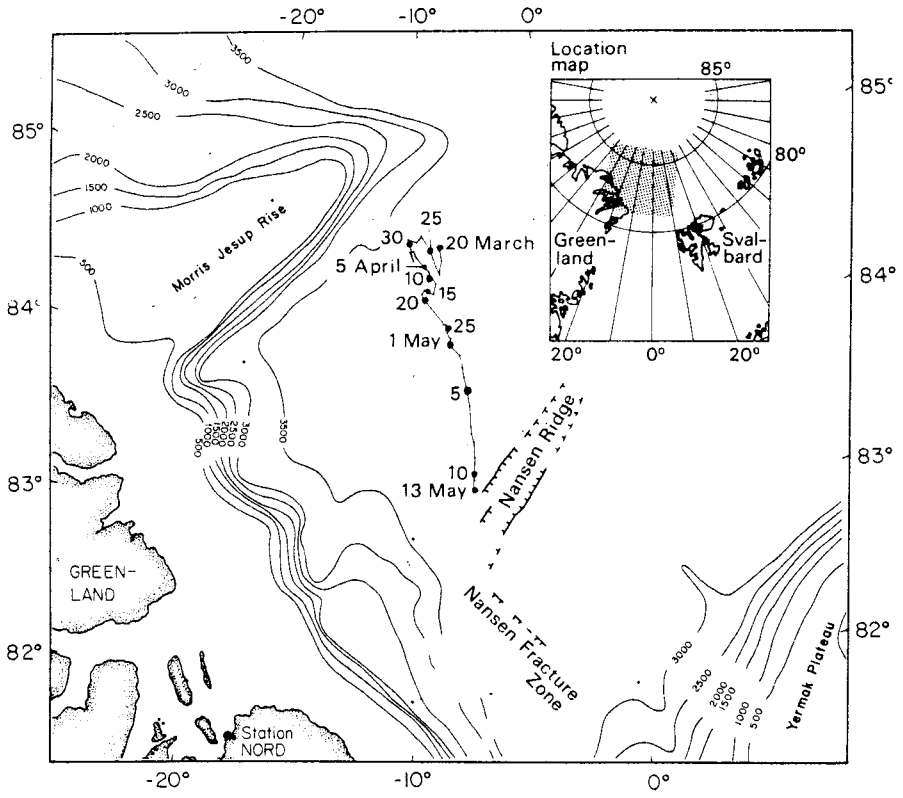

Fig. 1. Drift track of U.S. ice station FRAM I, 1979. Bathymetry in meters from GEBCO chart 5-17 (1979).

THE FRAM I MICROEARTHQUAKE EXPERIMENT

Six slightly modified AN-SSQ/41A sonobuoys were deployed on ice floes out to 4 km away from the FRAM-I main camp in the beginning of April 1979. The buoys were supplied with beam antennas and alkaline batteries sufficient for more than 3 months continuous operation. Holes were drilled in the floes and the buoys were placed ca. 0.2 m above water and covered with insulating material. The hydrophones were dropped through a second hole and suspended at 60 m depth. As the sea-water temperature is $-1.5°C$ and air temperatures in the range $-20°C$ to $-30°C$, the temperature near the ice–water interface is -5 to $-10°C$, which is well below the lower operating temperature threshold of $-2°C$ for the buoys. Nevertheless, three of the buoys provided useful signal quality throughout a 40-day period, while the buoys at the three other recording sites were operational for 10–20 days and had to be replaced. The maximum useful radio range of the buoys did not exceed 5 km, which is attributed to reduced output power at the low temperatures and/or poor grounding. The sonobuoy signals were received by retuned amateur band (145 MHz) receivers equipped with ± 25 kHz crystal filters and recorded on Sprengnether MEQ-800 microearthquake instruments. Sonobuoy transmitters as well as receivers had automatic gain control. Seismic refraction signals were recorded digitally on Sprengnether DR-100 event recorders. Spot depth soundings over the Nansen Ridge were made by helicopter landings and detonation of small charges. Also a Sprengnether MEQ-800 instrument was operated at Station Nord (NOR) in northeastern Greenland from March 21 to June 12, 1979, in conjunction with the FRAM I experiment.

A common problem in using sonobuoy arrays in the open ocean is accurate tracking of the position of individual buoys. The ice-covered Arctic Ocean, however, offers the advantage that the relative positions of buoys in an array remain fairly constant over periods ranging from days to several weeks. In our case, the array geometry was monitored by helicopter using a Motorola Mini-Ranger navigation system with two transponder sites positioned by Magnavox MX-1502 satellite receivers. The relative motion of individual buoys ranged from 20 to 350 m over the 6-weeks period and could be measured to within ± 5 m. Absolute positioning of the array was limited by the accuracy of individual satellite fixes, i.e., ± 100 m.

The sonobuoy array was operational for the 6-week period from April 1–May 13, 1979. Through the whole month of April the ice station was more than 100 km away from the Nansen spreading center, but drifted rapidly southwards at a rate of 12 km/day during the first 10 days of May (see Fig. 1). During the final days of manned operation, FRAM I drifted along the northwestern crest of Nansen Ridge at a rate of only 2 km/day to within 25 km of the median valley with concurrent low ambient noise levels in the water and favourable conditions for microearthquake recording.

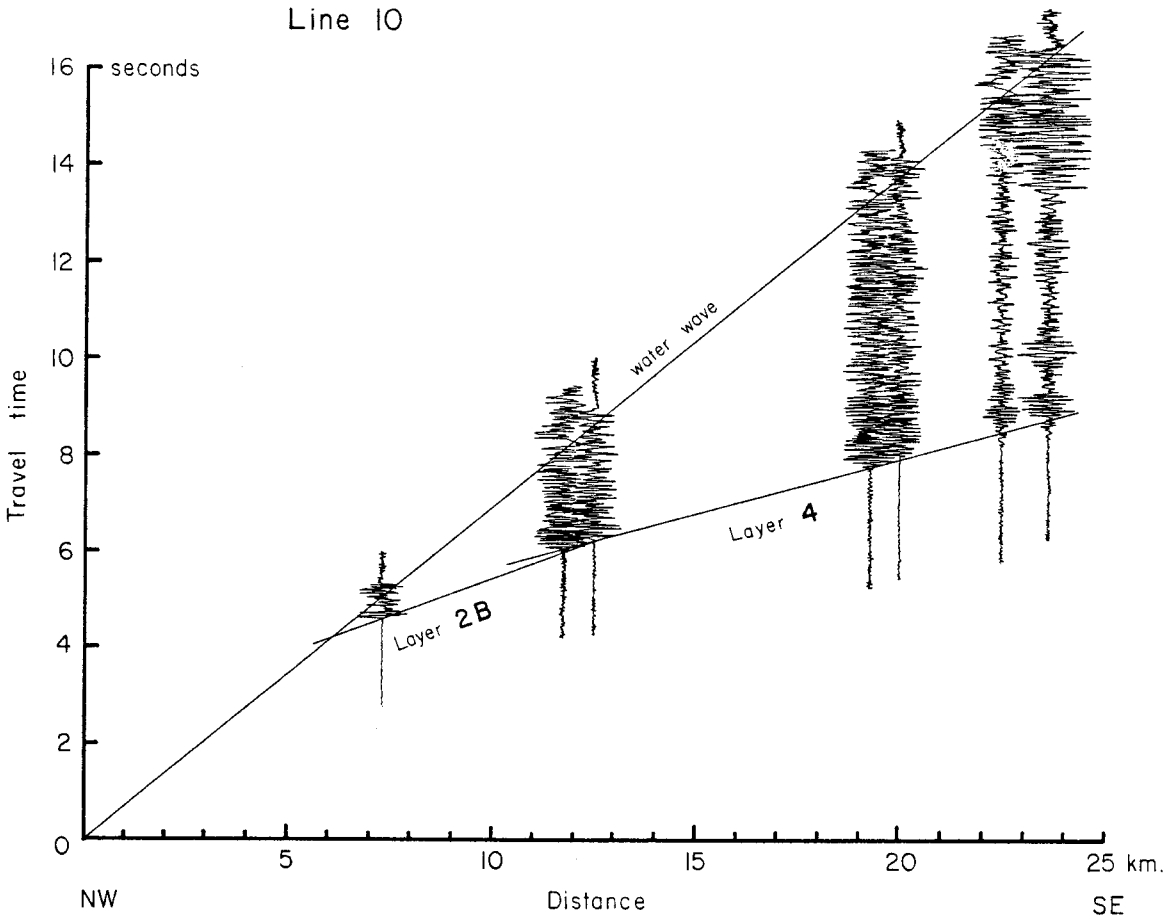
Line 10
seconds
Travel time
water wave
Layer 4
Layer 2B
NW
Distance
SE
25 km.

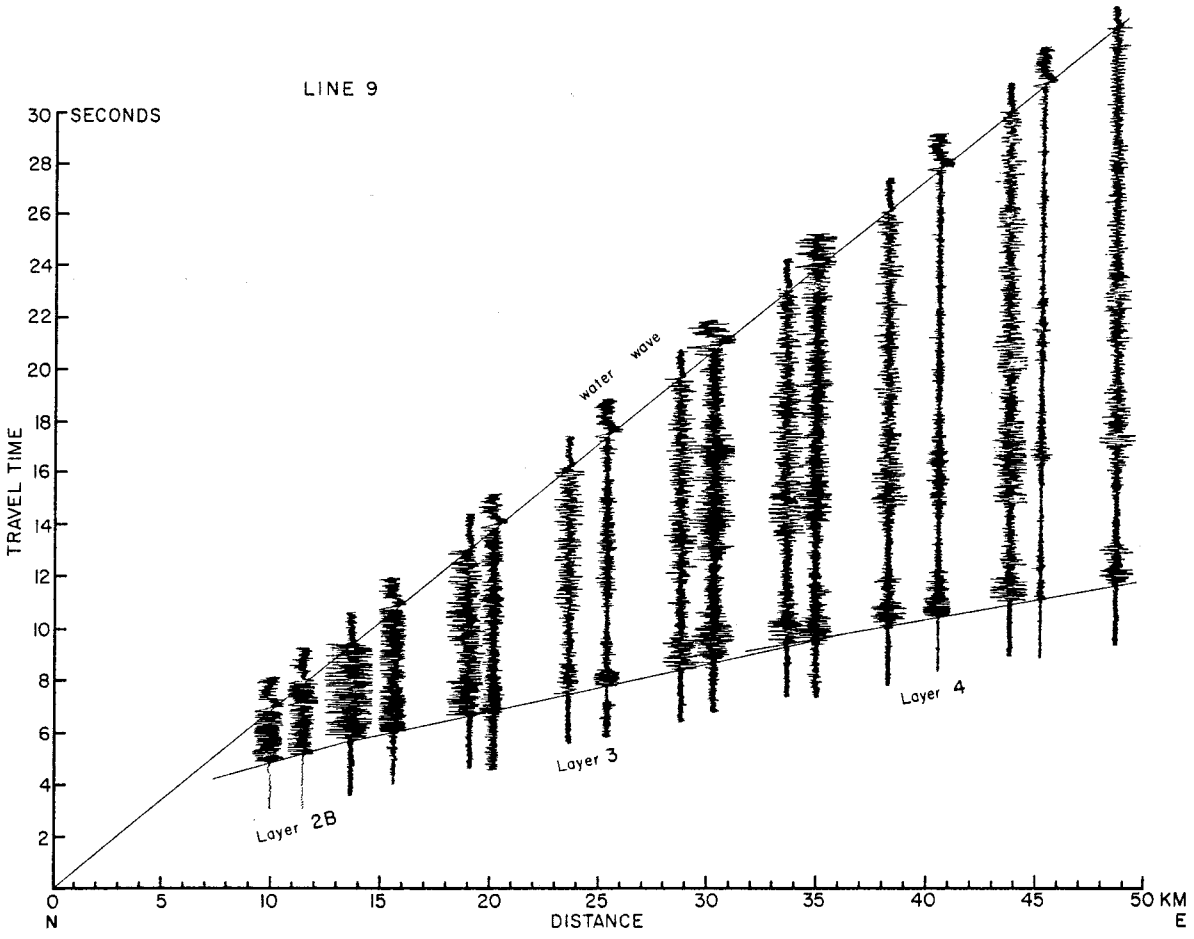
LINE 9
SECONDS
TRAVEL TIME
water wave
Layer 4
Layer 3
Layer 2B
DISTANCE
N
E
50 KM

DATA ANALYSIS AND RESULTS

Crustal structure

The FRAM I geophysics program comprised a series of unreversed seismic refraction measurements for mapping of the oceanic crustal velocity structure. Two profiles near the spreading center were particularly useful for establishing a crustal model for locating the recorded microearthquakes and some of the data are displayed in Fig. 2 (profile locations are shown in Fig. 5). Also, three helicopter traverses (shown in Fig. 5) with spot depth soundings were made in order to delineate the rift valley. Seismic signals were generated using charges ranging from 4 to 25 kg of TNT with depth-sensitive primers set for 100 m depth and dropped through the ice at 5 km intervals.

In a preliminary interpretation of the data, the crustal velocity structure has been approximated by few homogenous layers. The two refraction profiles (lines 9 and 10) closest to the Nansen spreading center show a velocity at the sea floor of 4.6 km/s (Fig. 3), but the results from line 10 are relatively uncertain as shooting was down the steep mountain side with an average slope of 5.8° into the rift valley. Under the crestal mountains (line 9) a 6.1 km/s refractor is observed at about 1.5 km depth overlying a 7.9 km/s velocity at 6 km below the sea floor. In the median valley a velocity of 7.2 km/s is observed at 3 km depth. These preliminary results are in good agreement with other studies from slow spreading ridges (see review by Spudich and Orcutt, 1980). Results of the seismic refraction program will be reported in a later paper.

Microearthquake activity

Until May 9 at least 20 seismic signals, likely to have originated from earthquake sources, were recorded by the sonobuoy array on FRAM I and 13 of these signals were also recorded by the microearthquake instrument at NOR. During the last 36 hours of operation, the ice station being about 25 km away from the median valley, 96 events were recorded. The wave trains characteristically have sharp P arrivals as well as S waves converted to P (SP) at the sea floor (Fig. 4). Dominant signal frequencies are in the 15–20 Hz range. For the nearest events (SP–P time of 4 sec or equivalent to 15 km epicentral distance) no direct water wave is observed, whereas more distant events exhibit a clear T phase arrival (Fig. 4). For the most distant

Fig. 2. a. Seismic refraction data line 9 along the northwestern flank of the Nansen Ridge. Shot ranges, measured by Motorola Mini-Ranger navigation system, are known to within ±20 m. Traces are lined up with respect to water wave arrival using sound velocity as a function of range given by Hunkins et al. (1969). Layer designation following Houtz and Ewing (1976). Profile location shown in Fig. 5. b. Seismic refraction data line 10. Other information as for Fig. 2a.

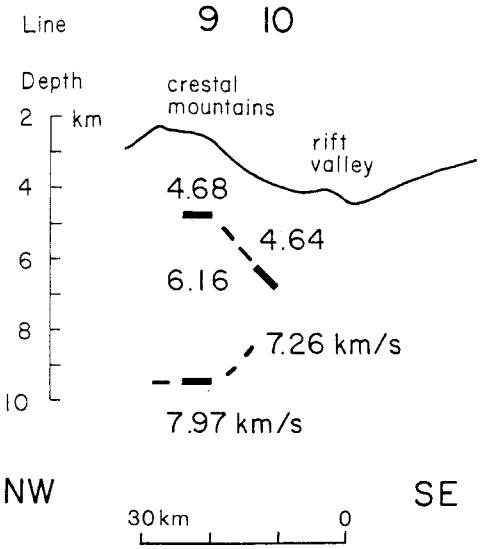

Fig. 3. Preliminary seismic compressional velocity structure of the northwestern flank of the Nansen Ridge using few homogenous layers. The following average model was used for epicenter location: water depth 2.3 km, compressional velocities for layer 2, 3 and 4 were 4.6 km/s, 6.1 km/s and 7.6 km/s, respectively, and the thicknesses for layers 2 and 3 were 2.6 km and 3.4 km, respectively. V_p/V_s ratio = 1.85 (Hyndman, 1979).

events recorded when the ice station was more than 100 km away from the ridge axis, SP-phases are less distinct because of attenuation.

Location of seismic events outside a microearthquake array poses significant stability problems in the computation of the epicenter parameters. The procedure used here is a modification of the classical S–P location method, and the approach is to obtain a preliminary solution from the difference in arrival times of SP and P waves. This is done by assigning a Gaussian uncertainty "ridge" to a segment of the distance circle near the cross-over point between circles and a maximum-likelihood

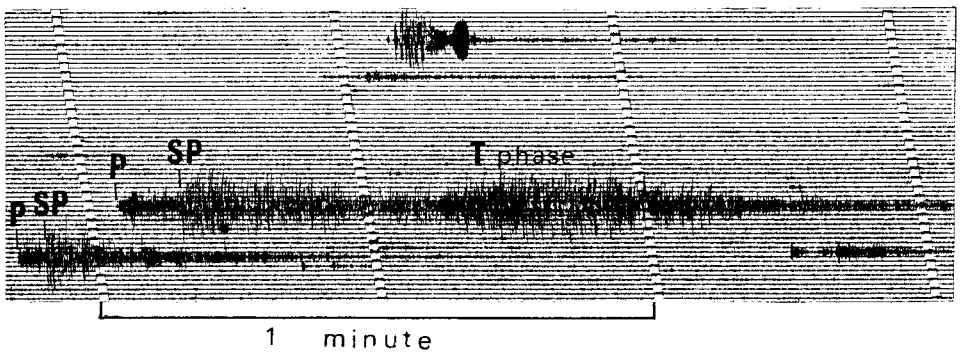

Fig. 4. Sample seismogram from May 12, 1979. Largest event shows strong, direct water-wave arrival (T phase), epicenter distance 50 km. Closer events show no T-phase (lower left event $\Delta = 15$ km). Characteristic recording of a signal which has travelled through the Arctic Ocean SOFAR channel is seen in the upper central part of seismogram (shot distance 700 km).

solution is found from the joint probabilities. Any number of stations can be added in this way, and theoretical P-wave travel-times are then compared to observed values and the process is iterated to minimize residuals. This location procedure has been successfully applied in a number of cases when standard programs such as HYP071 failed to converge (Bungum and Kristoffersen, 1980). Of the 69 events recorded 21 could be located using this procedure (Table I and Fig. 5). Focal depths have been restrained to 1 and 5 km below the sea floor to display the influence of assumed focal depth on epicenter location. Location errors are estimated to be about 1–2 km in the radial direction and 4–10 km in the tangential direction from the array. The majority of epicenters appear to line up closely with the location of the medial valley as outlined from spot soundings. It is interesting to note that several events with significantly shorter epicenter distances occurred on the northwestern flank of the rift valley.

Magnitudes are not calculated here, mainly because ground motions are difficult to retrieve from our data. Ambient noise levels in the ice-covered Arctic Ocean are less than 1 μbar in the frequency band 10–20 Hz during periods of no wind and

TABLE I

Located microearthquakes on the Nansen Ridge assuming focal depth 1 km below sea floor

Date	Hours	Lat. (°N)	Long. (°W)	NP *	RMS
790511	0259 13.0	83.43	4.88	4	0.04
790511	0301 30.7	83.42	4.82	4	0.03
790511	0306 11.8	83.42	4.82	4	0.04
790511	1806 01.2	83.38	5.57	4	0.10
790511	2234 01.4	83.25	5.48	6	0.15
790512	0149 56.2	83.33	4.82	4	0.17
790512	0159 03.5	83.22	5.29	6	0.12
790512	0449 56.7	83.33	4.72	4	0.09
790512	0454 47.2	83.39	4.56	4	0.15
790512	0718 29.3	83.30	5.81	6	0.04
790512	0829 48.9	83.21	5.27	6	0.11
790512	0836 40.3	83.45	4.88	5	0.14
790512	0854 34.1	83.30	5.00	6	0.17
790512	1640 15.9	83.28	4.94	4	0.04
790512	1925 17.0	83.33	5.60	6	0.12
790513	0043 15.9	83.23	5.17	6	0.13
790513	0221 27.5	83.27	4.87	6	0.21
790513	0340 39.4	83.32	5.00	6	0.18
790513	0416 12.2	83.21	5.27	5	0.02
790513	0416 28.2	83.26	5.83	6	0.07
790513	0710 07.3	83.12	5.89	4	0.06

* NP is number of phases used in location and RMS is root mean square of arrival time residuals in seconds.

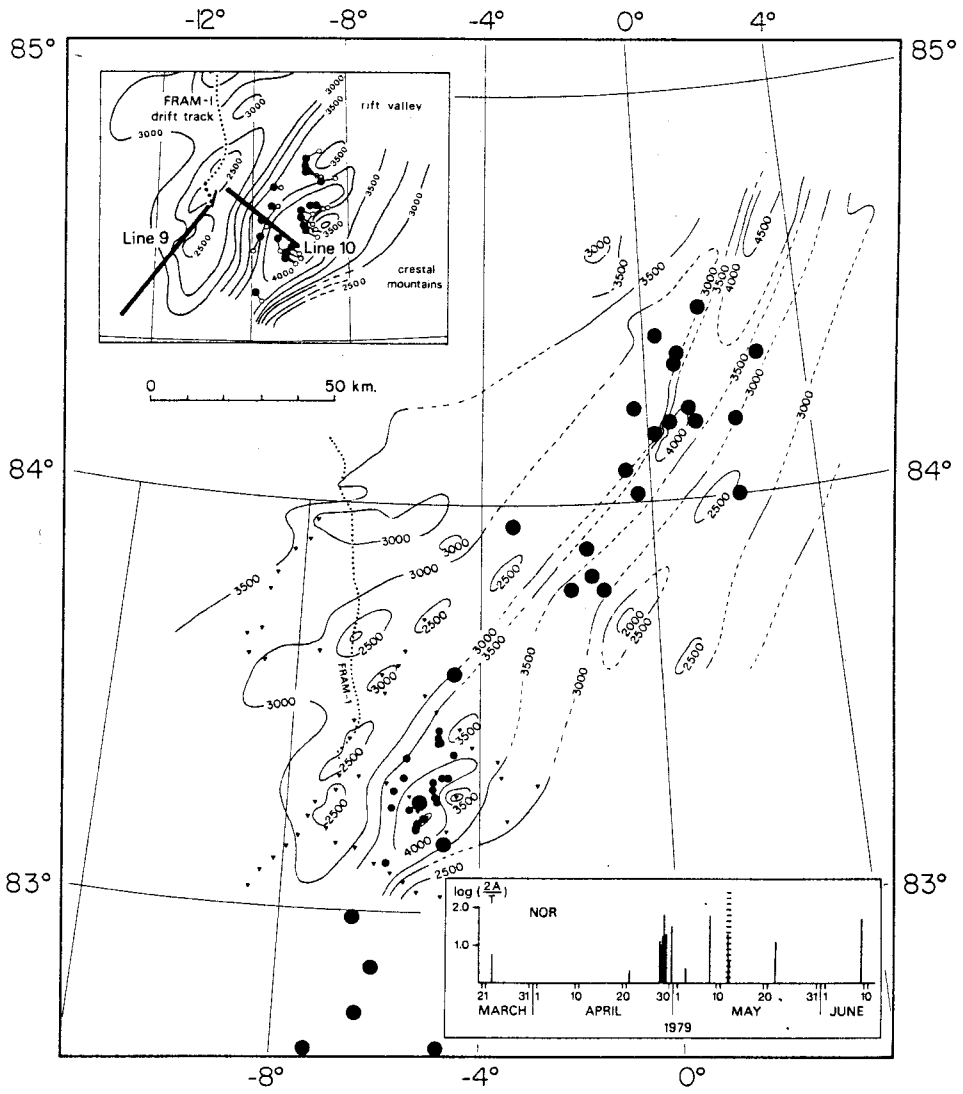

Fig. 5. Locations of microearthquakes recorded by FRAM I sonobuoy array (small dots) and teleseismically located earthquakes 1961–1979 (large dots) from International Seismological Centre (ISC) and U.S.G.S. Preliminary Determinations of Epicenters (PDE). Triangles mark locations of spot depth soundings. Bathymetry modified from GEBCO chart 5-17 (1979).

Upper left inset: Microearthquake locations for two assumed focal depths, 1 km (dots) and 5 km (open circles). The drift of the array during the recording interval is indicated by heavier dots, and line at the end of the track indicates sonobuoy array dimension. Heavy lines show locations of seismic refraction lines.

Lower right inset: Time sequence of earthquakes occurring in the southern part of the Nansen Ridge with signal amplitudes recorded at NOR, northeastern Greenland, illustrated by vertical bars. A is the maximum zero-to-peak signal amplitude in millimeters on the vertical component seismograph record and T the corresponding period in seconds. A term of approx. 2 should be added to the vertical scales for conversion into body wave magnitude. Shaded area indicates 36-hour recording interval at the ridge crest by sonobuoy array.

slow ice drift (H. Kutschale, pers. commun., 1980). A zero-magnitude earthquake would generate a pressure pulse of about 2.5 μbar at 20 Hz at a distance of 10 km (Reid et al., 1973). We therefore conservatively estimate our detection threshold to be around magnitude 1.

DISCUSSION

When the difference in epicenter distance is taken into account, it appears that the microearthquake activity on the Nansen Ridge observed from FRAM I is significantly higher than that observed on the Mid-Atlantic Ridge by Spindel et al. (1974) with a sonobuoy array at 36°30′N and Lilwall et al. (1978) at 45°N using ocean-bottom seismometers.

Earthquake locations from global networks (ISC and USGS PDE) show relatively few teleseismic events to have occurred since 1961 (Fig. 5). The frequency–magnitude distribution for these data shows that the teleseismic detectability drops significantly for magnitudes below 4.5. Assuming a slope of -1.0, we find that an upper limit for 15 years of earthquake activity from the areas in Fig. 5 is (cumulatively):

$$\log N = 5.8 - m_b$$

Assuming uniform earthquake distribution along the ridge, and a uniform distribution in time, this estimate can be scaled down to cover the FRAM I detection window in space and time (48 hours), i.e.:

$$\log N = 1.6 - m_b$$

We should therefore expect (at most) one $m_b = 1.6$ earthquake, 4 earthquakes above $m_b = 1.0$ and 40 above $m_b = 0.0$. Actually 69 events were recorded in 36 hours and all of these earthquakes appear to be above 1.0 in magnitude.

From the above considerations we have strong reasons to believe that our two days of recording actually cover a local swarm. This is also supported by results from NOR operating 200 km away. A total of 21 out of 60 earthquakes recorded at NOR during the period March 21–June 12 with S–P times between 18 and 24 s could be located using at least two of the stations: Nord, FRAM I, Danmarkshavn Greenland (DAG) or Ny-Ålesund Spitsbergen (KBS). The time sequence of 15 of these events which occurred on the Nansen Ridge around 81.3°N 6°W clearly shows a swarm in late April and early May (Fig. 5 lower right). Body wave magnitude of the largest event is estimated to be around $m_b = 4$ although none or at best very few of these events were large enough to be recorded at teleseismic distances.

The microearthquake locations on the Nansen Ridge show two parallel linear trends separated by about 10 km (Fig. 5). As noted earlier, we were unable to obtain independent focal depth estimates, although exitation of distinct *T*-phases by all events from the median valley favour shallow earthquake sources. The seismic activity within rift valleys appears to be restricted to the upper 7–8 km below the sea

floor (Jones and Johnson, 1978; Lilwall et al., 1978). Assuming a focal depth of 1 km for all events, one epicenter trend appears to coincide with the median valley and the other as a sequence of events located along the northwestern rift valley wall. Possible focal-depth differences between events do not change the epicenter locations significantly. If, however, the hypocenters of the trend aligned with the median valley were 5 km or deeper, their locations would be closer to the southeastern rift valley wall. Although focal depths are indeterminant, it is clear from Fig. 5 that this uncertainty will not affect the two epicenter lineations as such. The seismicity indicates active fault lengths of 25 km or more. More distant events in the median valley may not be detected if a low-velocity zone is present beneath the median valley. The seismic activity may, in the case of shallow events, possibly be attributed to movement of a fault block about 10 km wide being uplifted from the median valley to the rift valley wall. The greater number of events occurring in the median valley would then suggest differential movement between the two sides of the block or be related to intrusive and/or extrusive events in the median valley. If, however, the events occurred at a greater depth (5 km) they could have been associated with motion on fault systems on both sides of the median valley.

Although recording intervals are limited to a few days, other microearthquake studies in rift valley environments show a tendency for most of the seismic activity to be related to a single tectonic event—such as magma intrusion beneath the median valley (Lilwall et al., 1978), faulting at the base of the median valley wall (Spindel et al., 1974) or within the valley wall itself (Jones and Johnson, 1978). The data reported here is potentially the first observational evidence of a parallel epicenter system on a ridge segment suggesting motion of a fault block. Extensive long-range, side-scan sonar coverage from parts of the Mid-Atlantic Ridge indicates that most of the faulting occurs 2–4 km from the spreading center and no significant fault motion beyond the crestal mountains is evident from the sea-floor morphology (Laughton and Searle, 1979). Typical spacing between faults or clusters of faults is 2–2.5 km with fault lengths in the range 5–50 km.

The relatively uniform seismic activity (1–2 events/hour) observed here on the Nansen Ridge and by others elsewhere on the Mid-Atlantic Ridge contrasts with the tendency towards predominance of microearthquake swarm activity observed on segments of faster spreading ridges, such as on the Gorda Ridge (Jones and Johnson, 1978), in the Gulf of California (Reid et al., 1973) and on the Galapagos Ridge (Macdonald and Mudie, 1974).

CONCLUSIONS

Despite the harsh environment, the ever-present ice cover in the Arctic Ocean lends itself favourably to relatively inexpensive array-type marine geophysical experiments, as the rigidity of the ice greatly diminishes the relative motion between individual sensors and simplifies the navigational bookkeeping.

A small earthquake swarm occurring on the Nansen Ridge was recorded by a sonobuoy array during the FRAM I ice drift experiment. Two parallel linear epicenter trends about 25 km long occurred in the median valley and on the northwestern rift valley wall. This activity was probably related to uplift of a fault block from the median valley to the rift valley wall. Preliminary analysis of seismic refraction measurements from the crestal mountains of the Nansen Ridge indicates a velocity structure very similar to what is observed elsewhere on slow-spreading mid-ocean ridge segments.

ACKNOWLEDGEMENTS

We gratefully acknowledge the working spirit of Alf Nilsen, Josè Ardai and the helicopter crew: Helge Siljuberg and Gøran Lindmark, in the field. Ice station FRAM I was funded by Office of Naval Research, Arlington Va., as part of a long-term effort to improve our understanding of the submarine geology and tectonics of the Arctic Ocean. Norwegian scientific programs were coordinated and funded by the Norwegian Polar Research Institute, Oslo. Norsk Polarinstitutt Contribution No. 201.

REFERENCES

Barazangi, M. and Dorman, J., 1970. Seismicity map of the Arctic compiled form ESSA, Coast and Geodetic Survey, epicenter data January 1961 through September 1969. Bull. Seismol. Soc. Am., 60: 1741–1743.

Beal, M.A., 1969. Bathymetry and Structure of the Arctic Basin. Thesis, Oregon State University, Corvallis, Oreg. 204 pp.

Bungum, H. and Kristoffersen, Y., 1980. A microearthquake Survey of the Svalbard region. Final Report, Phase I. NTNF/NORSAR Tech. Rep/ No. 1/80: 28 pp.

Feden, R.H., Vogt, P.R. and Fleming, H.S., 1979. Magnetic and bathymetric evidence for the "YERMAK hot spot" northwest of Svalbard in the Arctic Basin. Earth Planet Sci. Lett., 44: 18–38.

Hunkins, K.L., Kutschale H.W., and Hall, J.K., 1969. Studies in marine geophysics and underwater sound from drifting ice stations. Lamont-Doherty Geol. Obs., Columbia Univ., Rep. No. 266 (82): 68 pp.

Hunkins, K., Kristoffersen, Y., Johnson, G.L. and Heiberg, A., 1979. The FRAM I Expedition. EOS, Trans. Am. Geophys. Union, 60: 1043–1044.

Hyndman, R.D., 1979. Poisson's ratio in the oceanic crust—a review. Tectonophysics, 59: 321–333.

Houtz, R. and Ewing, I., 1976. Upper crustal structure as a function of plate age. J. Geophys. Res., 81: 2490–2498.

Jones, P.R. and Johnson, S.H., 1978. Sonobuoy array measurements of active faulting on the Gorda Ridge. J. Geophys. Res., 83: 3455–3441.

Karasik, A.M., 1968. Magnetic anomalies of the Gakkel Ridge and origin of the Eurasia Subbasin of the Arctic Ocean. Geophys. Methods Prospect. Arctic, 5: 8–19.

Laughton, A.S. and Searle, R.C., 1979. Tectonic processes on slow spreading ridges. In: M. Talwani, C.G. Harrison and D.F. Hayes (Editors), Deep Drilling Results in the Atlantic Ocean: Ocean Crust. Am. Geophys. Union, Maurice Ewing Ser., 2: 15–33.

Lilwall, R.C., Francis, T.J.G. and Porter, I.T., 1978. Ocean-bottom seismograph observations on the Mid-Atlantic Ridge near 45°N—further results. Geophys. J.R. Astron. Soc., 55: 255–262.

Mcdonald, K.C. and Mudie, J.D., 1974. Microearthquakes on the Galapagos Spreading Center and the seismicity of fast-spreading ridges. Geophys. J.R. Astron. Soc., 36: 245–257.

Reid, I., Reichle, M., Brune, J. and Bradner, H., 1973. Microearthquake Studies Using Sonobuoys: Preliminary Results from the Gulf of California. Geophys. J.R. Astron. Soc., 34: 365–379.

Spindel, R.C., Davis, S.B., Macdonald, K.C. Porter, R.P. and Philips, J.D., 1974. Microearthquake survey of median valley of the Mid-Atlantic Ridge at 36°30′N. Nature, 248: 577–579.

Spudich, P. and Orcutt, J., 1980. A New Look at the Seismic Velocity Structure of the Oceanic Crust. J. Geophys. Res., 18(3): 627–645.

Sykes, L.R., 1965. Seismicity of the Arctic. Bull. Seismol. Soc. Am., 55: 501–518.

Vogt, P.R., Taylor, P.T., Kovacs, L.C. and Johnson, G.L., 1979a. Detailed Aeromagnetic Investigations of the Arctic Basin. J. Geophys. Res., 84: 1071–1089.

Vogt, P.R., Kovacs, L.C., Johnson, G.L. and Feden, R.H., 1979b. The evolution of the Arctic Ocean with emphasis on the Eurasian Basin. Proc. Norwegian Sea Symp., Nor. Pet. Soc., Oslo.